

Insights from experiment and *ab initio* calculations into the glasslike transition in the molecular conductor κ -(BEDT-TTF)₂Hg(SCN)₂Cl


Elena Gati,¹ Stephen M. Winter,^{1,2} John A. Schlueter,^{3,4} Harald Schubert,¹ Jens Müller,¹ and Michael Lang¹

¹Physikalisches Institut, J.W. Goethe-Universität Frankfurt(M), SFB/TR49, D-60438 Frankfurt(M), Germany

²Institut für Theoretische Physik, J.W. Goethe-Universität Frankfurt(M), SFB/TR49, D-60438 Frankfurt(M), Germany

³Division of Materials Research, National Science Foundation, Arlington, Virginia 22230, USA

⁴Materials Science Division, Argonne National Laboratory, Argonne, Illinois 60439, USA

 (Received 24 October 2017; revised manuscript received 20 December 2017; published 9 February 2018)

We present high-resolution measurements of the relative length change as a function of temperature of the organic charge-transfer salt κ -(BEDT-TTF)₂Hg(SCN)₂Cl. We identify anomalous features at $T_g \approx 63$ K which can be assigned to a kinetic glasslike ordering transition. By determining the activation energy E_A , this glasslike transition can be related to conformational degrees of freedom of the ethylene endgroups of the organic building block BEDT-TTF. As opposed to other κ -(BEDT-TTF)₂X salts, we identify a peculiar ethylene endgroup ordering in the present material in which only one of the two crystallographically inequivalent ethylene endgroups is subject to glasslike ordering. This experimental finding is fully consistent with our predictions from *ab initio* calculations from which we estimate the energy differences ΔE and the activation energies E_A between different conformations. The present results indicate that the specific interaction between the ethylene endgroups and the nearby anion layers leads to different energetics of the inequivalent ethylene endgroups, as evidenced by different ratios $E_A/\Delta E$. We infer that the ratio $E_A/\Delta E$ is a suitable parameter to identify the tendency of ethylene endgroups toward glasslike freezing.

DOI: [10.1103/PhysRevB.97.075115](https://doi.org/10.1103/PhysRevB.97.075115)

I. INTRODUCTION

Organic charge-transfer salts are considered as model systems in the study of the physics of strongly correlated electron systems in low dimensions [1–5]. They are outstanding by the variety of intriguing ground states, including superconductivity [6–8], Mott insulating [1,9,10], multiferroic [11,12] and spin-liquid states [13,14]. This diversity reflects a high tunability of interaction strength and frustration which can be accessed in laboratory environments by the application of moderate pressures or slight chemical modifications [1,15,16]. Besides that, organic charge-transfer salts are available in very clean single-crystalline form, as evidenced by the observation of quantum oscillations in low fields [17,18]. Nevertheless, these systems tend to be susceptible to intrinsic disorder, which arises from structural degrees of freedom of the large-sized molecular building blocks [19,20]. This type of intrinsic disorder occurs whenever a certain structural unit can adopt two different orientations which are almost degenerate in energy. In this situation, the structural elements often cannot order for kinetic reasons and instead tend to undergo glasslike transitions around a characteristic temperature T_g . The properties of this “glasslike” state in otherwise well-ordered solids are found to be similar [21,22] to conventional glass formers [23], i.e., undercooled liquids, such as glucose. The term glass implies that the relaxation of the structural degrees of freedom becomes so slow that thermal equilibrium cannot be reached and short-range structural order with residual disorder is “frozen.” An important characteristic of this glasslike behavior is that the conditions of the nonequilibrium state depend on the cooling rate [24]. Conversely, the amount of frozen disorder

can be very well controlled in a reversible way by varying the cooling rate. Thus, the organic charge-transfer salts have been identified as a suitable test ground to investigate the delicate interplay between strong electronic correlations and disorder effects [25–30], a problem that is relevant for any solid-state realization of a strongly correlated electron system and treated in theoretical models, such as the Mott-Anderson model [31–33].

Particularly well-suited materials for these investigations are members of the widely studied family of κ -(BEDT-TTF)₂X charge-transfer salts (X represents a monovalent anion, see Fig. 1) for the following reasons. First, this material class reflects the rich phenomenology associated with strong correlations [1,3], as represented by the multiferroic Mott insulator [1,11,34] $X = \text{Cu}[\text{N}(\text{CN})_2]\text{Cl}$, the superconductors [6] $X = \text{Cu}[(\text{NCN})_2]\text{Br}$ and $\text{Cu}(\text{SCN})_2$, and the spin-liquid candidate system [13] $X = \text{Cu}_2(\text{CN})_3$. Second, structural degrees of freedom, susceptible to glasslike ordering, are inherent to the molecular building block BEDT-TTF which stands for $\text{C}_6\text{S}_8[\text{C}_2\text{H}_4]_2$ (bis-ethylenedithio-tetrathiafulvalene). Here, the ethylene endgroups $[\text{C}_2\text{H}_4]$ (abbreviated as EEG hereafter) can adopt two different relative orientations [see Fig. 1(c)], either an eclipsed (E) or a staggered (S) one when viewed along the central C = C bond. The population of these two conformations is often thermally disordered at room temperature, with a tendency to adopt one of the configurations upon lowering the temperature T (see Refs. [24,26] for an overview). Whereas the salt $X = \text{Cu}_2(\text{CN})_3$ does not reveal any signatures of a glasslike ordering [35,36] of the EEGs at low T , despite thermal disorder at room temperature, the three other salts mentioned above all undergo glasslike transitions [37–39]

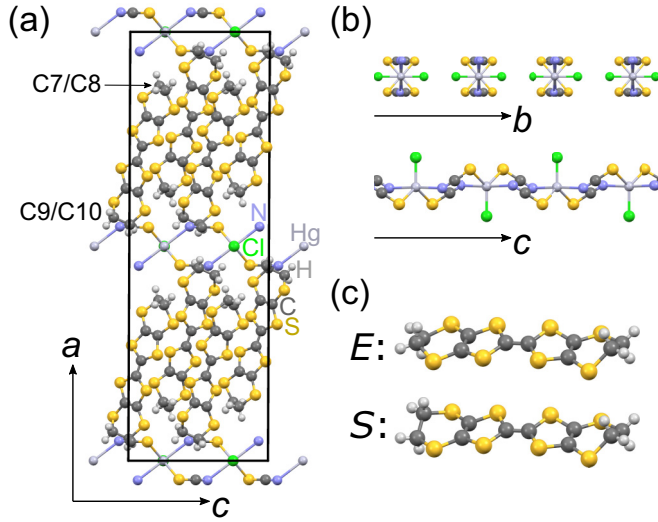


FIG. 1. Structure of κ -(BEDT-TTF) $_2$ Hg(SCN) $_2$ Cl: (a) alternating layers of (BEDT-TTF) $_2^+$ and (Hg(SCN) $_2$ Cl) $^-$ along the out-of-plane a axis. C7/C8 and C9/C10 refer to the carbon atoms of the two crystallographically inequivalent ethylene endgroups in the present material which we label with inner and outer EEGs, respectively; (b) polymeric anion layer (Hg(SCN) $_2$ Cl) $^-$ viewed along the in-plane b and c axes, indicating the dominant chainlike character along the c axis; (c) orientational degrees of freedom of the ethylene endgroups (EEGs) of the BEDT-TTF molecule. E refers to the eclipsed configuration, S to the staggered configuration.

around $T_g \approx 70$ K. Various experiments demonstrated that the dynamics of the EEGs [40] strongly affect the ground-state properties of these salts. In particular, the properties of the two superconducting salts $X = \text{Cu}[\text{N}(\text{CN})_2]\text{Br}$ and $\text{Cu}(\text{SCN})_2$, including their critical temperature [27,41–43] T_c , were found to be strongly sensitive on the cooling procedure through T_g . In case of the former salt $X = \text{Cu}[\text{N}(\text{CN})_2]\text{Br}$, it was even possible to reversibly tune the system from a metal to a Mott insulator [44,45] by increasing the cooling rate $|q|$. Recently, it was argued that this large effect cannot solely be attributed to the effects of disorder, but also to changes of the interaction strength [45,46] which result from different hopping energies in the eclipsed and staggered configuration.

This strong influence of the orientational degrees of freedom of the EEGs on the physical properties motivates the interest in understanding and modeling the EEG behavior. It is likely and also found experimentally that the details of the EEG ordering depend on the specific system. This concerns not only the preferred orientation at low T , but also the occurrence of a glasslike transition: As indicated by the examples given above, only a few, but not all κ -(BEDT-TTF) $_2X$ salts, undergo a glasslike transition. In a comparative experimental and theoretical *ab initio* study by Müller *et al.* [26] on a wide range of κ -(BEDT-TTF) $_2X$ salts, it was argued that the distinct behavior can be explained consistently by considerations of the energetics of the different conformations. Importantly, the energies are mostly determined by the specific anion-EEG interaction. This emphasizes that not only EEG degrees of freedom are involved in the glasslike ordering process, but also their coupling to the anions [47] leading to a collective

motion of EEG and anion molecules that freezes at T_g [26]. For the first time, these calculations allow to make predictions on the occurrence of a glassy EEG state in the κ -(BEDT-TTF) $_2X$ salts.

In this paper, we apply these theoretical methods to the charge-ordered [48] ferroelectric [49] salt κ -(BEDT-TTF) $_2$ Hg(SCN) $_2$ Cl and identify it as a special candidate for understanding the mechanisms of glasslike EEG ordering. We predict only half of the EEGs undergo a glasslike transition, whereas the other half is predicted to order smoothly. Such a distinct behavior in one single system was not resolved yet for any other κ -(BEDT-TTF) $_2X$ salt. To verify this theoretical prediction for κ -(BEDT-TTF) $_2$ Hg(SCN) $_2$ Cl, we conduct measurements of the thermal expansion coefficient on this salt to unravel the potential glasslike EEG ordering. This technique was successfully used in the past to identify glasslike ordering in κ -phase organic charge-transfer salts [39]. The high sensitivity of this method is due to its inherent sensitivity to structural variations.

II. METHODS

Single crystals of κ -(BEDT-TTF) $_2$ Hg(SCN) $_2$ Cl were synthesized by the standard electrocrystallization technique. We followed the strategy reported in Ref. [50], however with minor modifications of the synthesis route, as follows. Pure TCE (1,1,2-Trichloroethane) was employed as a solvent with a mixture of Hg(SCN) $_2$ and PPnCl (bis(triphenylphosphoranylidene)ammonium chloride) in a molar ratio of 1:1 serving as the electrolytes. The electrolyte was given in a ten-fold excess to the solution in relation to the BEDT-TTF. This results in a typical composition of 75 mg of BEDT-TTF, 642 mg of Hg(SCN) $_2$ and 1132 mg of PPnCl in 100 ml solvent. A constant current of 0.2 μA was applied to platinum electrodes, resulting in a voltage of 0.1 V – 0.3 V. Crystal growth was performed at a temperature of 20°C and crystals were collected after 4 – 5 weeks. Crystals were characterized by means of resistance measurements to identify the characteristic metal-insulator transition [51] in this compound at $T_{\text{MI}} \approx 30$ K. For the thermal expansion measurements, the crystals were oriented by eye resulting in a maximum misalignment of 5°.

Measurements of the relative length change $\Delta L_i(T)/L_i$ ($i = a, b, c$), with $\Delta L_i(T) = L_i(T) - L_i(T_0)$ and T_0 a reference temperature (here chosen to be $T_0 = 200$ K), were performed by using a home-built capacitive dilatometer. The design of this dilatometer is similar to the one described in Ref. [52] and reaches a maximum sensitivity of $\Delta L/L \approx 10^{-10}$. The thermal expansion coefficient

$$\alpha_i(T) = \frac{1}{L_i} \frac{dL_i}{dT} \quad (1)$$

$$\approx \frac{1}{L_i(300 \text{ K})} \frac{\Delta L_i(T_2) - \Delta L_i(T_1)}{T_2 - T_1}, \quad (2)$$

$$\text{with } T = (T_1 + T_2)/2 \text{ and } i = a, b, c, \quad (3)$$

was calculated numerically from the $\Delta L_i(T)/L_i$ data using the following procedure: The $\Delta L_i(T)/L_i$ data were divided into equidistant intervals of typically $\Delta T = 0.3$ K. In each of these intervals the mean slope was determined from a linear

regression. The mean slope together with the mean temperature in this interval correspond to one data point in the α_i versus T representation. Measurements of $\Delta L_i(T)/L$ [and correspondingly $\alpha_i(T)$] were performed upon warming and cooling in the temperature range $5 \text{ K} \leq T \leq 200 \text{ K}$. The temperature was controlled by a LakeShore 340 controller using a heating rate of $q_h = +1.5 \text{ K/h}$ and cooling rates ranging between $(1.20 \pm 0.05) \text{ K/h} \leq |q_c| \leq (20.7 \pm 0.3) \text{ K/h}$.

Ab initio calculations were performed using ORCA [53] at the B3LYP/def2-SV(P) level, based on the structural data at $T = 300 \text{ K}$ reported in Ref. [48], and following the procedure from Ref. [26]. In particular, the positions of the EEGs were relaxed, while the remaining atoms were fixed. We stress that temperature-induced thermal expansion effects do not lead to significant changes in the resulting energy scheme. The interaction between the dimer and anion layer were approximated via the OPLS-aa forcefield [54], with Lennard-Jones parameters from the GROMACS set [55]. The anion charge distribution was estimated from Mulliken analysis of B3LYP/def2-SV(P) calculations on small fragments. For transition-state calculations, ORCA's hessian mode following algorithm was employed.

III. THEORY: *AB INITIO* CALCULATIONS

A two-level model is often used to describe glasslike transitions [24] [see Fig. 2(a)]. In this model, two states with energy difference $2\Delta E$ are separated by an activation barrier of size E_A leading to a thermally activated relaxation time $\tau \propto \exp[E_A/(k_B T)]$. In the following, we discuss possible conformations of the EEGs in κ -(BEDT-TTF)₂Hg(SCN)₂Cl and our computational results on the energy scheme in a simple two-level model, including $2\Delta E$ and E_A . We distinguish the inequivalent EEGs within each dimer by their distance to the anion layer [see Fig. 1(a)]: The outer EEGs (containing carbon atoms C9 and C10) almost penetrate the anion layer, whereas the inner ones (carbon atoms C7 and C8) are shifted away from the anion layer. In contrast to κ -(BEDT-TTF)₂Cu[N(CN)₂]Z ($Z = \text{Br}, \text{Cl}$), both the inner and outer EEGs are disordered [48] at room temperature in κ -(BEDT-TTF)₂Hg(SCN)₂Cl. This gives rise to four possible EEG conformations within each molecule in the latter compound (sixteen total conformations for each dimer). The majority conformation at room temperature sees both molecules in a staggered orientation that we denote as $S(1)$, shown in Fig. 1(a). The other three molecular conformations are labeled with $E(1)$, $E(2)$, and $S(2)$ and are obtained by changing the orientation of the inner [$E(1)$], the outer [$E(2)$; Fig. 2(b)], or both EEGs [$S(2)$]. The 16 total conformations of each dimer are then obtained as different combinations of these four molecular conformations. According to recent structural investigations [48], the inner EEGs are significantly more disordered at room temperature than the outer EEGs: This results in distinctly higher occupancies of the molecular conformations $S(1)$ and $E(1)$ of 43% and 35% (>25%), respectively, compared to occupancies of 12% for $E(2)$ and 10% for $S(2)$ (<25%).

To explore the relative stability of the various conformations, we estimated the energies of the various conformations of κ -(BEDT-TTF)₂Hg(SCN)₂Cl via *ab initio* calculations as outlined in Sec. II. In agreement with the results of structure

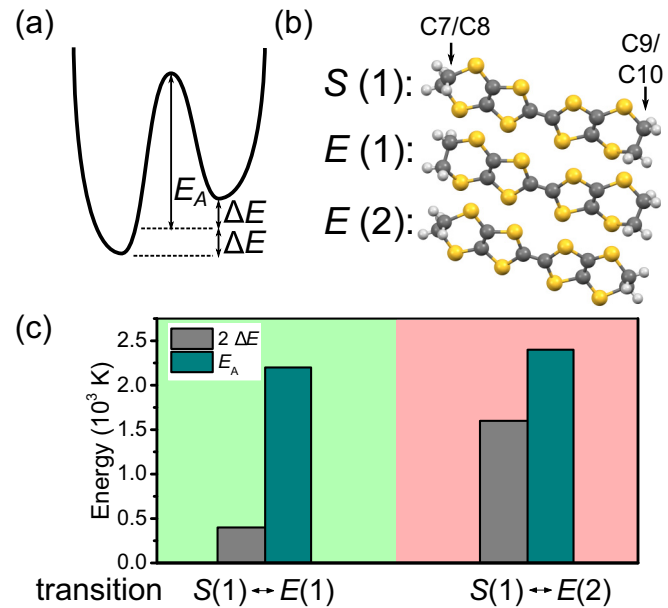


FIG. 2. (a) Schematic two-level system in which two states with energy difference $2\Delta E$ are separated by an activation barrier E_A ; (b) view on BEDT-TTF molecules in three different ethylene endgroup (EEG) conformations, which can be realized in κ -(BEDT-TTF)₂Hg(SCN)₂Cl. The majority conformation is a staggered conformation, labeled as $S(1)$. The configuration $E(1)$ [$E(2)$] is obtained from $S(1)$ by changing the orientation of the inner EEGs containing carbon atoms C7 and C8 (outer EEGs containing carbon atoms C9 and C10); (c) computed energy values $2\Delta E$ and E_A for the processes $S(1) \leftrightarrow E(1)$ and $S(1) \leftrightarrow E(2)$ in κ -(BEDT-TTF)₂Hg(SCN)₂Cl. The green background color indicates that our calculations predict a glasslike transition for this process, the red background color indicates that no glasslike transition is predicted.

determination [48], our calculations yield that $S(1)$ is the most stable molecular conformation. From this starting point, we considered the energy cost E_i to convert one molecule from $S(1)$ to the $E(1)$, $E(2)$, and $S(2)$ conformation. After averaging over all dimer conformations according to the experimental room temperature occupancies (see Supplemental Material for details [56]), we find energy differences $2\Delta E_i$ [see Fig. 2(c)]:

$$2\Delta E_{E(1)} = |E_{E(1)} - E_{S(1)}| = (400 \pm 100) \text{ K},$$

$$2\Delta E_{E(2)} = |E_{E(2)} - E_{S(1)}| = (1600 \pm 200) \text{ K},$$

$$2\Delta E_{S(2)} = |E_{S(2)} - E_{S(1)}| = (1900 \pm 200) \text{ K},$$

where the variance indicates the weighted standard deviation of the computed values. These relative energies are in line with the experimentally determined occupancies of the different conformations; those conformations with lower experimental room-temperature occupancy are found to have higher energies.

The relative stability of the different conformations is strongly influenced by the interactions of the EEGs with the nearby anion layer. In κ -(BEDT-TTF)₂Hg(SCN)₂Cl, the nonplanar polymeric anions [see Fig. 1(b)] form a chainlike structure that consists of Hg^{2+} containing polymers with bridging $(\text{SCN})^-$ ligands and short-side chains formed by

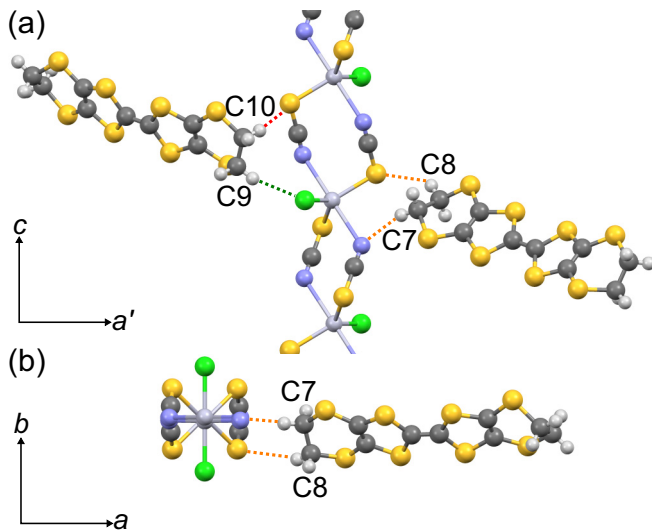


FIG. 3. Preferred ethylene endgroup (EEG) conformation [staggered $S(1)$] relative to the nearby anion layer for κ -(BEDT-TTF) $_2$ Hg(SCN) $_2$ Cl, viewed within the $a'c$ plane (a) and the ab plane (b). a' indicates a small rotation of the a axis around the c axis. Green and brown dashed lines indicate close contacts of the outer EEGs (labeled with C9 and C10) to the Cl and (SCN) ligands in the nearby anion layer. Orange lines indicate close contacts of the inner EEGs (labeled with C7 and C8) to the (SCN) ligands in the nearby anion layer.

the terminal ligand Cl^- coordinated to each Hg^{2+} . The two inequivalent EEGs of each BEDT-TTF molecule are embedded in a distinct local environment leading to different coupling paths between the EEGs and the anions [see Fig. 3(a)]: The inner EEGs (with carbon atoms C7 and C8) possess only close (SCN) \cdots H contacts. In contrast, the outer EEGs couple to the anion via (SCN) \cdots H and Cl \cdots H contacts. The large $2\Delta E_i$ values for $i = E(2)$ and $S(2)$, which both involve a change of the orientation of the outer EEGs suggest that this EEG conformation is rigidly confined by the coupling to the anion layer. In contrast, the (SCN) \cdots H interaction to the inner EEGs seems to be rather ineffective in energetically distinguishing the two orientations, as represented by a comparably small $2\Delta E_{E(1)} = 330$ K. Thus, the inner EEGs are closer to a metastable state than the outer EEGs.

From transition-state calculations, we also estimated activation energies [see Fig. 2(c)] for the transition from $S(1)$ to $E(1)$ to be $E_{A,1} \approx 2200$ K and for the transition from $S(1)$ to $E(2)$ to be $E_{A,2} \approx 2400$ K. We note that we omit a discussion of the process $S(1) \leftrightarrow S(2)$, as this transition involves changing the orientation of both EEGs. Assuming now that the behavior of the two EEGs in one BEDT-TTF molecule can be considered independently, this implies that the process $S(1) \leftrightarrow S(2)$ can be decomposed into a two-step transition via an intermediate eclipsed conformation. Thus, the behavior of this process is either dominated by the process $S(1) \leftrightarrow E(1)$ or $S(1) \leftrightarrow E(2)$. The given values for $E_{A,i}$ are in the range of E_A values obtained for other κ -(BEDT-TTF) $_2$ X salts ($2000 \text{ K} \leq E_A \leq 3100 \text{ K}$), determined by various thermodynamic and transport experiments [34,38,39,57] as well as by *ab initio* calculations [26]. In Ref. [26] it was argued that glasslike freezing occurs

whenever two conformations are similar in energy compared to the activation energy of their interchange, i.e., whenever the ratio $E_A/\Delta E$ is sufficiently large. Based on a comparative study of the computed $E_A/\Delta E$ ratios for various κ -phase BEDT-TTF salts, a threshold value [26] of $E_A/\Delta E \gtrsim 5$ was found empirically. For κ -(BEDT-TTF) $_2$ Hg(SCN) $_2$ Cl, we find $E_{A,1}/\Delta E_{E(1)} \sim 11$ for the inner EEGs and $E_{A,2}/\Delta E_{E(2)} \sim 3$ for the outer EEGs [see Fig. 2(c)]. We note that $E_{A,1}/\Delta E_{E(1)}$ is the largest ratio among all investigated κ -(BEDT-TTF) $_2$ X salts [26] emphasizing the large metastability of this conformation. Applying the empirical threshold proposed in Ref. [26], the calculations predict only one glasslike transition in the inner EEGs—despite the existence of two inequivalent EEGs with potential for glassy freezing. The outer EEGs are expected to order smoothly as for $X = \text{Cu}_2(\text{CN})_3$.

IV. EXPERIMENT: THERMAL EXPANSION MEASUREMENTS

A. Phenomenology of glasslike transitions in thermal expansion measurements

Before discussing the salient results of our thermal expansion studies on the organic charge-transfer salt κ -(BEDT-TTF) $_2$ Hg(SCN) $_2$ Cl, we first introduce the main signatures of glasslike transitions in thermodynamic quantities (see also Ref. [39] for a detailed discussion). To study thermal equilibrium properties, the experimental observation time Δt has to be much larger than the relaxation time of the system τ , i.e., $\Delta t \gg \tau$. If this criterion is violated, nonequilibrium phenomenon are observed. This is the case for glass (and glasslike) transitions in which the relaxation time of a system slows down so dramatically with lowering T that the relaxation time τ can reach the value of the observation time Δt . Then equilibrium conditions cannot be reached anymore and a glass transition into a metastable state with short-range order occurs at T_g . The long relaxation time of the system beyond experimental observation times affects thermodynamic properties in the following ways:

(1) As the associated motion is frozen on experimental timescales below T_g , it does not contribute to thermodynamic quantities, such as the specific heat $C(T)$ or the thermal expansion coefficient $\alpha(T)$. In contrast, above T_g these degrees of freedom can be thermally excited and therefore contribute additionally to $C(T)$ and $\alpha(T)$. As a consequence, a steplike increase of $C(T)$ and steplike changes [58] of $\alpha(T)$ at T_g are expected upon warming.

(2) In contrast, the cooling behavior of a glass-forming system is expected to be distinctly different from the warming behavior resulting in a strong thermal hysteresis. Whereas upon cooling a smooth anomaly is expected, the discontinuous steplike feature upon warming is usually accompanied by characteristic over- and undershoots. This behavior reflects the strong tendency of a system to achieve an equilibrium state as soon as T_g is approached from below.

(3) Last, the behavior of the system is strongly dependent on the cooling rate. In particular, the glass transition temperature T_g is strongly affected. On the one hand, the faster a system is cooled, the smaller is the experimental observation time Δt . On the other hand, the relaxation time increases with lowering

T . Correspondingly, the criterion $\Delta t \approx \tau$ is fulfilled at higher temperatures and T_g increases with cooling rate $|q|$. Given the definition of $q = \Delta T/\Delta t$, the glass transition temperature can be defined based on the criterion $\Delta t \approx \tau$ as follows [22,59]:

$$-|q| \left. \frac{dT}{d\tau} \right|_{T_g} \simeq 1. \quad (4)$$

The three main characteristics listed above clearly discriminate a glass transition from a thermodynamic phase transition which takes place in equilibrium.

B. Results

Now we will turn to the experimental results of the relative length change $\Delta L_i(T)/L_i$ and the thermal expansion coefficient $\alpha_i(T) = L_i^{-1} dL_i/dT$ on κ -(BEDT-TTF)₂Hg(SCN)₂Cl. Figure 4 shows $\Delta L_i(T)/L_i$ (a) and $\alpha_i(T)$ (b) along all three crystallographic axes $i = a, b, c$ over a wide temperature range $5 \text{ K} \leq T \leq 200 \text{ K}$, taken upon warming. At low temperatures $T \approx 30 \text{ K}$, $\Delta L_i(T)/L_i$ shows a jump of the length in all crystallographic directions, implying a divergent $\alpha_i(T)$. At this temperature, κ -(BEDT-TTF)₂Hg(SCN)₂Cl undergoes a transition from a low-temperature charge-ordered insulating state to a high-temperature metallic state [48,51]. Accordingly, we assign this feature to the signature of the metal-insulator transition and label this transition temperature with T_{MI} . However, the study of the metal-insulator transition is not in the focus of the present work and will be discussed in detail elsewhere [49]. Upon warming, a second anomaly can be identified at $T \approx 63 \text{ K}$. At this temperature, we observe kinklike anomalies in $\Delta L_i(T)/L_i$ along all three crystallographic axes. These anomalies are reflected by steplike features in $\alpha_i(T)$ [see Fig. 4(b)]. As will be discussed below, the anomalies in $\alpha_i(T)$ can be assigned to glasslike ordering of the EEGs around a characteristic temperature of $T_g \approx 63 \text{ K}$. We note that our directional-dependent studies of $\Delta L_i(T)/L_i(T)$ and $\alpha_i(T)$ reveal a strongly anisotropic behavior around T_g . The expansivities α_a and α_b are positive below and above T_g . This corresponds to a usual increase of the length with increasing T , however, with an abrupt change of slope around T_g [see Fig. 4(a)]. In contrast, the length along the c axis is increasing with increasing temperature for $T < T_g$ and decreasing with temperature for $T > T_g$, giving rise to a sign change of $\alpha_c(T)$ around T_g . We stress that the almost null effect in $\Delta L_c/L_c$ along the c axis, observed between $T \approx 80 \text{ K}$ and 200 K is consistent with the results of previously published x-ray diffraction data [48] at room temperature and $T = 100 \text{ K}$. The unusual decrease of $\Delta L_c/L_c$ with increasing T observed in the present work is commonly called “negative thermal expansion,” abbreviated as NTE. It persists up to $T \approx 140 \text{ K}$, as revealed by a turning point in $\Delta L_c(T)/L_c$, tantamount to the sign change in $\alpha_c(T)$. A possible origin for this phenomenon in the present salt will be discussed below. First, we present further experimental data on the anomalous contribution to $\alpha_i(T)$ around $T_g \approx 63 \text{ K}$.

Figure 5(a) shows a closer look on the thermal expansion coefficient $\alpha_c(T)$, which demonstrates the strongest effect around the glasslike transition at $T_g \approx 63 \text{ K}$. This data set was collected upon slowly warming ($q_h = +1.5 \text{ K/h}$ after cool

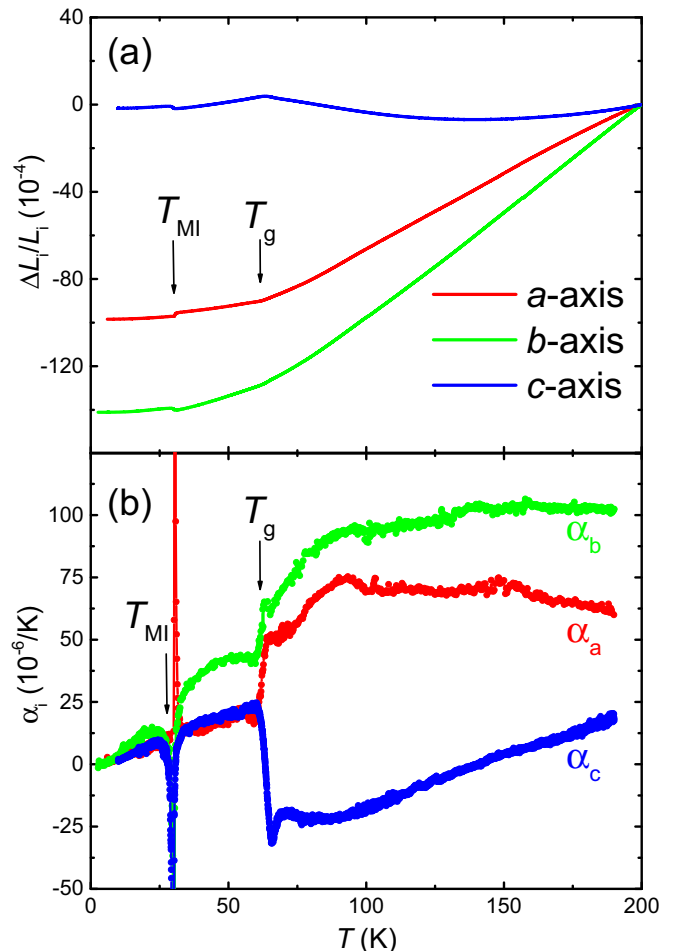


FIG. 4. Relative length change $\Delta L_i(T)/L_i$ normalized to the reference temperature $T_0 = 200 \text{ K}$ (a) and thermal expansion coefficient $\alpha_i(T) = L_i^{-1} dL_i/dT$ (b) of the organic charge-transfer salt κ -(BEDT-TTF)₂Hg(SCN)₂Cl upon slow warming ($q_h = +1.5 \text{ K/h}$) after slow cooling ($q_c = -3 \text{ K/h}$). Red line corresponds to data taken along the out-of-plane $i = a$ axis, green and blue line to data along the in-plane $i = b$ and c axis, respectively. The anomalous kinks in $\Delta L_i(T)/L_i$ and the steplike features in $\alpha_i(T)$ at $T_g \approx 63 \text{ K}$ can be assigned to signatures of the glasslike transition (see main text for a detailed discussion). The jumps in $\Delta L_i/L_i$ and the divergent behavior in $\alpha_i(T)$ at $T_{\text{MI}} \approx 30 \text{ K}$ are related to a charge-order metal-insulator transition the investigation of which is not in the focus of the present study and will be discussed in detail elsewhere [49].

down with $q_c = -3 \text{ K/h}$, red closed circles) as well as upon slowly cooling ($q_c = -1.2 \text{ K/h}$, blue open circles). Upon warming, the steplike feature discussed above is accompanied by characteristic over- and undershoots of α_c at the low- and high-temperature flank of the anomaly, respectively. In contrast, these over- and undershoots are absent upon cooling. Instead, $\alpha_c(T)$ shows a strongly broadened steplike increase. Further away from T_g , the data taken upon warming and cooling fall on top of each other. The thermal hysteresis observed here marks an important experimental proof for the glassy nature of the anomaly and rules out a thermodynamic phase transition.

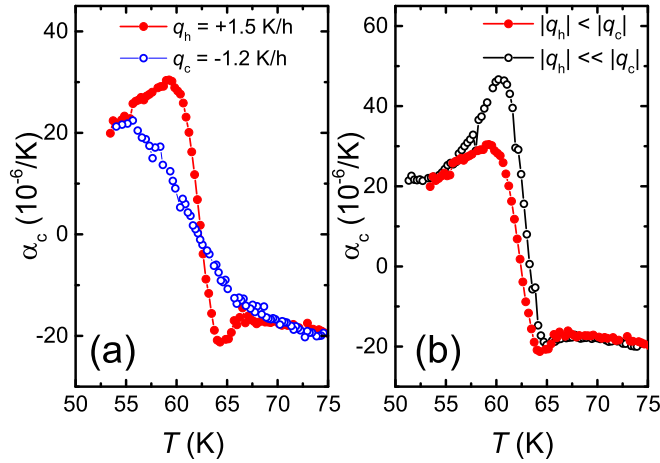


FIG. 5. Thermal expansion coefficient $\alpha_c(T)$ of κ -(BEDT-TTF)₂Hg(SCN)₂Cl measured along the in-plane c axis around $T_g \approx 63$ K: (a) hysteresis between data taken upon slow warming ($q_h = +1.5$ K/h, red closed circles) and data taken upon slow cooling ($q_c = -1.2$ K/h, blue open circles); (b) data taken upon slow warming ($q_h = +1.5$ K/h) after different cooling procedures: red closed circles represent data after slow cooling ($q_c = -3$ K/h), black open circles represent data taken after fast cooling ($q_c = -20.7$ K/h).

Furthermore, another characteristic aspect for glass-forming systems is the dependence of the expansivity on the cooling q_c and warming q_h rates. This relates, on the one hand, to (i) the explicit form of the anomaly and, on the other hand, to (ii) the $T_g(q)$ dependence. Concerning aspect (i), we present in Fig. 5(b) two data sets of $\alpha_c(T)$ which were measured upon heating ($q_h = 1.5$ K/h) after distinctly different cool-down procedures, i.e., after slow cooling with $q_c = -3$ K/h (red closed circles) and after comparably fast cooling with $q_c = -20.7$ K/h (black open circles). Both data sets reveal a steplike anomaly with over- and undershoot characteristics. Besides the significant shift of the anomaly to higher temperatures upon increasing $|q_c|$ [aspect (ii)], which will be discussed in more detail below the overshoot behavior at the low-temperature side of the anomaly is distinctly larger after fast cooling with $|q_c| = 20.7$ K/h than after slow cooling with $|q_h| \lesssim |q_c| = 3$ K/h. This is a direct signature of the relaxational phenomena close to T_g , which are more pronounced when the glass-forming system is cooled fast $|q_c| \gg q_h$ and the low- T frozen state is, thus, more disordered.

Finally, to discuss aspect (ii), i.e., the cooling-rate dependence of T_g , we present in Fig. 6(a) data of $\alpha_c(T)$ upon cooling using different cooling rates in the range -1.2 K/h $\leq q_c \leq -20.7$ K/h. It is evident that the anomalous sign change of α_c at $T = T_g$ [see Fig. 5(a)], shifts to higher T with increasing $|q_c|$. This is expected for a glass-forming systems in which the relaxation time τ increases with lowering T . To evaluate this shift quantitatively, we determine T_g at a given q_c by using the midpoint of the broad steplike features and include the information of the inverse glass-transition temperature T_g^{-1} versus $|q|$ in an Arrhenius-like fashion in Fig. 6(b). In this representation, the data follow a linear behavior, indicating a thermally activated relaxation time $\tau \propto \exp[E_A/(k_B T)]$. The slope of a linear fit to the present data set can be related to the

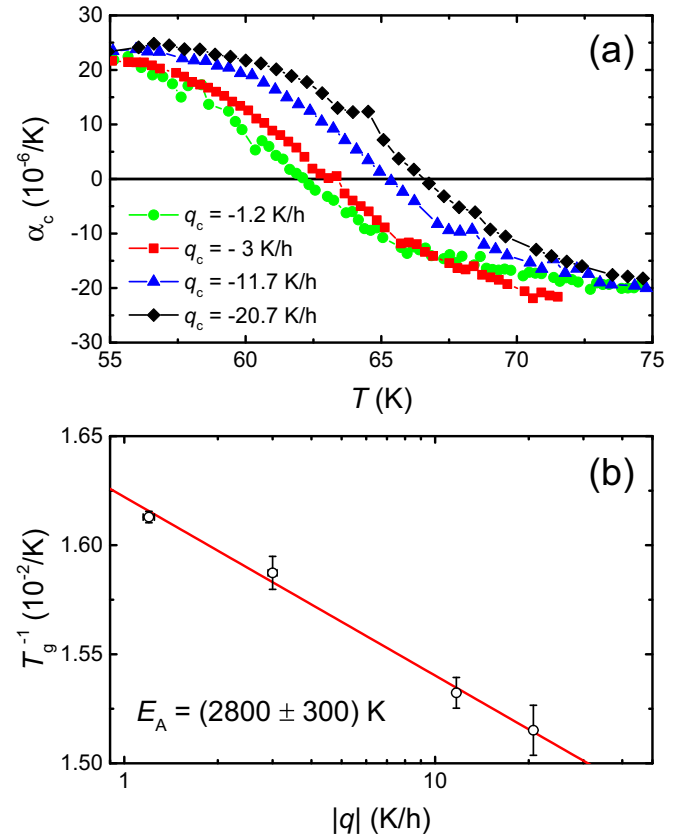


FIG. 6. Cooling-rate dependence of the glasslike transition temperature $T_g(|q|)$ and determination of the activation energy E_A : (a) Thermal expansion coefficient $\alpha_c(T)$ of κ -(BEDT-TTF)₂Hg(SCN)₂Cl measured along the in-plane c axis upon cooling using different cooling rates $-(1.2 \pm 0.05)$ K/h $\leq q_c \leq -(20.7 \pm 0.3)$ K/h; (b) Arrhenius plot of T_g^{-1} vs. $|q|$, yielding an activation energy of $E_A = (2800 \pm 300)$ K (for details of the analysis, see main text).

size of the activation energy barrier E_A in a simple two-level model with thermally activated relaxation time τ , as outlined in Refs. [39] and [59], via

$$\ln |q| = -\frac{E_A}{k_B T_g} + \text{const.} \quad (5)$$

In the present case, a linear fit [see red line in Fig. 6(b)] yields an estimate of the activation barrier energy $E_A = (2800 \pm 300)$ K. We stress that using this simple Arrhenius-type two-level model for the determination of the activation energy only provides a first estimate of the activation energy. In general, it is known in glass-forming systems that the activation energy can be strongly temperature dependent, in particular close to T_g . This temperature dependence is typically described in terms of the so-called Vogel-Fulcher-law. The results of Ref. [26] indeed reveal that the Vogel-Fulcher-law describes the dynamics of the EEGs in other κ -(BEDT-TTF)₂X salts more accurately in a wide frequency range of at least three orders of magnitude. However, in the present case, only a small frequency range (4×10^{-5} Hz $\lesssim f \lesssim 5 \times 10^{-4}$ Hz) is accessible due to the experimentally limited maximal cooling rate. In this range, the Arrhenius law and the Vogel-Fulcher-law

describe the data equally well, and thus the Arrhenius law is suitable for the determination of E_A .

V. DISCUSSION

The results of the thermal expansion measurements, in particular the steplike contribution to $\alpha_i(T)$ at $T_g \approx 63$ K, the thermal hysteresis and the strong cooling-rate dependence of T_g provide clear evidence for a glasslike transition in κ -(BEDT-TTF)₂Hg(SCN)₂Cl. From the determination of the activation energy $E_A = (2800 \pm 300)$ K, we can unequivocally assign the glasslike transition to an ordering of the EEGs [26,34,38,39]. Importantly, we find evidence for *only one* glasslike transition in the present compound despite the existence of two inequivalent EEGs with potential for thermal disorder. In case both EEGs would undergo a glasslike transition they would likely freeze at different temperatures T_g , as observed in κ -(BEDT-TTF)₂Cu(SCN)₂ [39]. This observation of only one glasslike transition is fully consistent with our predictions from *ab initio* calculations, presented above, in which we identified that only the conformations $S(1)$ and $E(1)$ (related to orientational degrees of freedom of the inner EEGs) are close to metastability, but not the conformations $E(2)$ and $S(2)$. Consequently, we assign the anomalies in $\alpha_i(T)$ to the glassy freezing of the inner EEGs. We note that for other κ -(BEDT-TTF)₂ X salts the activation energies E_A determined from thermal expansion measurements were found to be slightly larger than the computed values [26]. Keeping this in mind, the experimentally determined activation energy of $E_A = (2800 \pm 300)$ K is fully consistent with the computed value of $E_A = 2210$ K for the process $S(1) \leftrightarrow E(1)$ (see more detailed discussion below). We stress that our conclusion can be substantiated by structure determination [48] down to $T = 100$ K, which found that the inner EEGs exhibit disorder at this temperature, whereas the outer EEGs are fully ordered. However, we refrain from a comparison with published x-ray diffraction data at $T < 100$ K, as they were taken at a different instrument than the high-temperature structural data, thereby limiting the possibility of a comparison.

Our directional-dependent thermal expansion studies $\alpha_i(T)$ with $i = a, b, c$ reveal that the freezing of the inner EEGs is accompanied by strongly anisotropic lattice responses, which are particularly pronounced along the out-of-plane a and the in-plane c axis. The anomalous lattice contributions $\Delta\alpha_i(T_g) = \alpha_i(T \rightarrow T_g^+) - \alpha_i(T \rightarrow T_g^-)$ [see Fig. 4(b)] amount to $\Delta\alpha_a(T_g) = +(31 \pm 2) 10^{-6}/\text{K}$, $\Delta\alpha_b(T_g) = +(13 \pm 4) 10^{-6}/\text{K}$, and $\Delta\alpha_c(T_g) = -(42 \pm 2) 10^{-6}/\text{K}$. From a thermodynamic point of view, the $\Delta\alpha_i(T_g)$ values are related to the change of entropy associated with the EEG freezing S_{ethy} upon application of uniaxial pressure [39] along the i axis via

$$\left. \frac{\partial S_{\text{ethy}}}{\partial p_i} \right|_{T_g} = -V_{\text{mol}} \Delta\alpha_i(T_g). \quad (6)$$

By using the molar volume [48] $V_{\text{mol}} = 519 \text{ cm}^3$, we expect the strongest response of S_{ethy} for uniaxial pressures along the in-plane c axis, for which $\partial S_{\text{ethy}}/\partial p_c = +(2.1 \pm 0.1) \text{ J}/(\text{mol K kbar})$ corresponding to an increase of ethylene disorder for increasing uniaxial pressure p_c . We note that in a

simple two-level model the entropy is $S_{\text{ethy}}^{\text{max}} = 11.6 \text{ J}/(\text{mol K})$ at maximum, implying that the entropy is increased by 20% of $S_{\text{ethy}}^{\text{max}}$ by a uniaxial pressure of 1 kbar. This extraordinary pressure sensitivity of S_{ethy} emphasizes the strong metastability of the inner EEG conformation which is suggested by the large $E_A/\Delta E$ obtained in our calculations.

The relative ordering of $|\Delta\alpha_i|$ (with $|\Delta\alpha_c| > |\Delta\alpha_a| > |\Delta\alpha_b|$) is likely related to the directional nature of the short contacts between the inner EEGs and (SCN)⁻ ligands. The displacement vectors associated with these contacts have components primarily in the ac -plane, such that application of pressure along the a or c axis more strongly influences the EEG-anion interactions, and thus the relative stability of the various conformations. This observation strengthens the viewpoint that the coupling to the anions plays an important role in selecting the preferred EEG conformation.

The negative thermal expansion along the c axis (along the anionic chain direction) that precedes the glasslike transition is also particularly remarkable. A similar effect was also reported for the glass-forming salt κ -(BEDT-TTF)₂Cu[N(CN)₂]Br [47,60]. A plausible scenario is that transverse displacements of the ligands within the ab -plane—away from the chain axis—cause a shrinkage along the length of the chain [60–62]. This behavior is commonly known as the Poisson effect. We note that the NTE along the c axis is accompanied by an increase in length upon warming along the other two axes, thus indicating that transverse displacements take place. Taken together with the absence of a NTE below T_g , the observation of the NTE above T_g supports the notion that the collective EEG-anion motion [47] freezes out at T_g rather than an individual EEG rotation. This finding is consistent with insights from fluctuation spectroscopy experiments [26] which revealed non-Arrhenius-like slow dynamics, characteristic for a fragile glass former. It was argued that this implies a significant cooperativity between the EEGs which is most likely mediated by EEG-anion interactions. Indeed, such cooperativity effects might explain the small deviation of the experimentally determined activation energy $E_A \approx 2800$ K from the calculated one ($E_A \approx 2200$ K) in the present compound κ -(BEDT-TTF)₂Hg(SCN)₂Cl. Whereas the calculations do not take cooperativity effects into account, we determine the activation energy experimentally close to T_g where cooperativity is potentially important and might cause non-Arrhenius-like dynamics. We stress that the present thermodynamic approach does not allow for an analysis of E_A far above T_g . However, from the above-mentioned fluctuation spectroscopy experiments it is known that cooperativity tends to increase the activation barrier energy, likely due to the increased number of correlated molecules. In that sense, the larger experimental value of E_A compared to the calculated one suggests that cooperativity among the EEGs, mediated by the anions, leads to a fragile glass-forming state in the present material.

After the detailed analysis of the EEG behavior in κ -(BEDT-TTF)₂Hg(SCN)₂Cl, we would like to shortly address why tuning the EEG behavior in this compound could potentially provide important new insights into the physics of dimerized molecular conductors. In a recent study [49] on the present compound, we provided evidence for electronic ferroelectricity of order-disorder type which originates from

charge order within the dimer. We related the occurrence of charge order to a moderate degree of dimerization. Thus, the present material bridges the gap between strongly dimerized materials, often approximated as dimer-Mott systems at 1/2 filling, and non- or weakly dimerized systems at 1/4 filling exhibiting charge order. This conclusion emphasizes the role of the dimerization strength as an important parameter in the field of molecular conductors. Importantly, our present study of the thermal expansion around the glasslike transition suggests that different cooling procedures through T_g can strongly modify the molecular arrangement in the BEDT-TTF plane. Thereby, the intra- and interdimer hopping terms, which are the parameters relevant for the electronic structure, are mainly affected. This could potentially be used for tuning the dimerization strength. Likewise, the magnetic frustration ratio, found to be particularly large in the present compound, might be subject to changes induced by different EEG conformations.

VI. SUMMARY

In conclusion, by employing measurements of the thermal expansion, we provide clear evidence for a glasslike ordering transition at $T_g \approx 63$ K in the organic charge-transfer salt κ -(BEDT-TTF)₂Hg(SCN)₂Cl. Similar to other κ -(BEDT-TTF)₂X salts, orientational degrees of freedom of the ethylene endgroups (EEGs) of the BEDT-TTF molecule were identified to be responsible for the glassy behavior. In this regard, the present salt κ -(BEDT-TTF)₂Hg(SCN)₂Cl is special as the two inequivalent EEGs behave distinctly different, as one of them orders smoothly, whereas the other one freezes in a glassy manner. This result is consistent with *ab initio* calculations,

which estimate energy differences ΔE and activation energies E_A for the different conformations. Distinctly different interactions between the inequivalent EEGs and the anions lead to one metastable state, as evidenced by a large ratio $E_A/\Delta E$, and one strongly confined state with small $E_A/\Delta E$. Thus, our results confirm the concept proposed in Ref. [26] that $E_A/\Delta E$ is a suitable parameter to quantify the tendency of a system toward glasslike ordering. The identification of the peculiar EEG ordering in κ -(BEDT-TTF)₂Hg(SCN)₂Cl confirms that the interaction between the EEGs and the anions is the decisive factor for the occurrence of glasslike freezing in the κ -(BEDT-TTF)₂X organic charge-transfer salts. As the EEG vibrational degrees of freedom are known to couple strongly to the electronic degrees of freedom in this material class, it is interesting to investigate in the future how ground state properties of the strongly correlated electron system in κ -(BEDT-TTF)₂Hg(SCN)₂Cl are influenced by the presence of two EEG subsystems with distinctly different temperature-dependent vibrational properties.

ACKNOWLEDGMENTS

We acknowledge useful discussions with Benedikt Hartmann. Research performed in Frankfurt was supported by the German Science Foundation via the Transregional Collaborative Research Center SFB/TR49: Condensed Matter Systems with Variable Many-Body Interactions. S.M.W. thanks NSERC Canada for a postdoctoral fellowship. J.A.S. acknowledges support from the Independent Research and Development program while serving at the NSF.

-
- [1] K. Kanoda, *Hyperfine Interact.* **104**, 235 (1997).
 [2] T. Ishiguro, K. Yamaji, and G. Saito, *Organic Superconductors* (Springer, Berlin, 1998).
 [3] N. Toyota, M. Lang, and J. Müller, *Low-Dimensional Molecular Metals* (Springer, Berlin, 2007).
 [4] A. Lebed, *The Physics of Organic Superconductors and Conductors* (Springer, Berlin, 2008).
 [5] B. J. Powell and R. H. McKenzie, *Rep. Prog. Phys.* **74**, 056501 (2011).
 [6] M. Lang and J. Müller, *Organic Superconductors* (Springer, Berlin, Heidelberg, 2004).
 [7] J. Wosnitzer, *J. Low Temp. Phys.* **146**, 641 (2007).
 [8] G. Saito and Y. Yoshida, *Chem. Rec.* **11**, 124 (2011).
 [9] F. Kagawa, K. Miyagawa, and K. Kanoda, *Nature* **436**, 534 (2005).
 [10] E. Gati, M. Garst, R. Manna, U. Tutsch, B. Wolf, L. Bartosch, H. Schubert, T. Sasaki, J. Schlueter, and M. Lang, *Sci. Adv.* **2**, e1601646 (2016).
 [11] P. Lunkenheimer, J. Müller, S. Krohns, F. Schrettle, A. Loidl, B. Hartmann, R. Rommel, M. de Souza, C. Hotta, J. Schlueter *et al.*, *Nat. Mater.* **11**, 755 (2012).
 [12] M. Lang, P. Lunkenheimer, J. Müller, A. Loidl, B. Hartmann, N. H. Hoang, E. Gati, H. Schubert, and J. A. Schlueter, *IEEE Trans. Magn.* **50**, 2700107 (2014).
 [13] Y. Shimizu, K. Miyagawa, K. Kanoda, M. Maesato, and G. Saito, *Phys. Rev. Lett.* **91**, 107001 (2003).
 [14] T. Itou, A. Oyamada, S. Maegawa, M. Tamura, and R. Kato, *Phys. Rev. B* **77**, 104413 (2008).
 [15] S. Lefebvre, P. Wzietek, S. Brown, C. Bourbonnais, D. Jérôme, C. Mézière, M. Fourmigué, and P. Batail, *Phys. Rev. Lett.* **85**, 5420 (2000).
 [16] A. Kawamoto, K. Miyagawa, and K. Kanoda, *Phys. Rev. B* **55**, 14140 (1997).
 [17] J. Wosnitzer, *Fermi Surfaces of Low-Dimensional Organic Metals and Superconductors* (Springer-Verlag, Berlin, Heidelberg, 1996).
 [18] M. V. Kartsovnik, in *Layered Organic Conductors in Strong Magnetic Fields* (Springer, Berlin, Heidelberg, 2008), pp. 185–246.
 [19] J. P. Pouget and S. Ravy, *J. Phys. I France* **6**, 1501 (1996).
 [20] S. Ravy, R. Moret, and J. P. Pouget, *Phys. Rev. B* **38**, 4469 (1988).
 [21] J. Müller, *Chem. Phys. Chem.* **12**, 1222 (2011).
 [22] F. Gugenberger, R. Heid, C. Meingast, P. Adelman, M. Braun, H. Wühl, M. Haluska, and H. Kuzmany, *Phys. Rev. Lett.* **69**, 3774 (1992).
 [23] P. G. Debenedetti and F. H. Stillinger, *Nature* **410**, 259 (2001).
 [24] B. Hartmann, J. Müller, and T. Sasaki, *Phys. Rev. B* **90**, 195150 (2014).

- [25] T. Sasaki, *Crystals* **2**, 374 (2012).
- [26] J. Müller, B. Hartmann, R. Rommel, J. Brandenburg, S. M. Winter, and J. A. Schlueter, *New J. Phys.* **17**, 083057 (2015).
- [27] J. G. Analytis, A. Ardavan, S. J. Blundell, R. L. Owen, E. F. Garman, C. Jeynes, and B. J. Powell, *Phys. Rev. Lett.* **96**, 177002 (2006).
- [28] T. Sasaki, N. Yoneyama, Y. Nakamura, N. Kobayashi, Y. Ikemoto, T. Moriwaki, and H. Kimura, *Phys. Rev. Lett.* **101**, 206403 (2008).
- [29] K. Sano, T. Sasaki, N. Yoneyama, and N. Kobayashi, *Phys. Rev. Lett.* **104**, 217003 (2010).
- [30] S. Diehl, T. Methfessel, U. Tutsch, J. Müller, M. Lang, M. Huth, M. Jourdan, and H.-J. Elmers, *J. Phys.: Condens. Matter* **27**, 265601 (2015).
- [31] H. Shinaoka and M. Imada, *Phys. Rev. Lett.* **102**, 016404 (2009).
- [32] H. Shinaoka and M. Imada, *J. Phys. Soc. Jpn.* **78**, 094708 (2009).
- [33] K. Byczuk, W. Hofstetter, and D. Vollhardt, *Phys. Rev. Lett.* **94**, 056404 (2005).
- [34] K. Miyagawa, A. Kawamoto, Y. Nakazawa, and K. Kanoda, *Phys. Rev. Lett.* **75**, 1174 (1995).
- [35] R. S. Manna, M. de Souza, A. Brühl, J. A. Schlueter, and M. Lang, *Phys. Rev. Lett.* **104**, 016403 (2010).
- [36] H. O. Jeschke, M. de Souza, R. Valentí, R. S. Manna, M. Lang, and J. A. Schlueter, *Phys. Rev. B* **85**, 035125 (2012).
- [37] K. Saito, H. Akutsu, and M. Sorai, *Solid State Commun.* **111**, 471 (1999).
- [38] H. Akutsu, K. Saito, and M. Sorai, *Phys. Rev. B* **61**, 4346 (2000).
- [39] J. Müller, M. Lang, F. Steglich, J. A. Schlueter, A. M. Kini, and T. Sasaki, *Phys. Rev. B* **65**, 144521 (2002).
- [40] Y. Kuwata, M. Itaya, and A. Kawamoto, *Phys. Rev. B* **83**, 144505 (2011).
- [41] X. Su, F. Zuo, J. A. Schlueter, A. M. Kini, and J. M. Williams, *Phys. Rev. B* **58**, R2944(R) (1998).
- [42] T. F. Stalcup, J. S. Brooks, and R. C. Haddon, *Phys. Rev. B* **60**, 9309 (1999).
- [43] O. J. Taylor, A. Carrington, and J. A. Schlueter, *Phys. Rev. B* **77**, 060503 (2008).
- [44] B. Hartmann, D. Zielke, J. Polzin, T. Sasaki, and J. Müller, *Phys. Rev. Lett.* **114**, 216403 (2015).
- [45] J. Müller, B. Hartmann, and T. Sasaki, *Philos. Mag.* **97**, 3477 (2017).
- [46] D. Guterding, R. Valentí, and H. O. Jeschke, *Phys. Rev. B* **92**, 081109 (2015).
- [47] A. U. B. Wolter, R. Feyerherm, E. Dudzik, S. Stülow, C. Strack, M. Lang, and D. Schweitzer, *Phys. Rev. B* **75**, 104512 (2007).
- [48] N. Drichko, R. Beyer, E. Rose, M. Dressel, J. A. Schlueter, S. A. Turunova, E. I. Zhilyaeva, and R. N. Lyubovskaya, *Phys. Rev. B* **89**, 075133 (2014).
- [49] E. Gati, J. Fischer, P. Lunkenheimer, D. Zielke, S. Köhler, F. Kolb, H.-A. K. von Nidda, S. M. Winter, H. Schubert, H.-A. K. von Nidda *et al.*, [arXiv:1711.07384](https://arxiv.org/abs/1711.07384) (2017).
- [50] S. V. Konovalikhin, G. V. Shilov, O. A. D'yachenko, R. N. Lyubovskaya, M. Z. Aldoshina, and R. B. Lyubovskii, *Bull. Russ. Acad. Sci. Divis. Chem. Sci.* **41**, 704 (1992).
- [51] S. Yasin, E. Rose, M. Dumm, N. Drichko, M. Dressel, J. Schlueter, E. Zhilyaeva, S. Torunova, and R. Lyubovskaya, *Physica B* **407**, 1689 (2012).
- [52] R. Pott and R. Scheffczyk, *J. Phys. E: Sci. Instrum.* **16**, 444 (1983).
- [53] F. Neese, *Wiley Interdisc. Rev.: Comput. Mol. Sci.* **2**, 73 (2012).
- [54] W. L. Jorgensen and J. Tirado-Rives, *J. Am. Chem. Soc.* **110**, 1657 (1988).
- [55] S. Pronk, S. Páll, R. Schulz, P. Larsson, P. Bjelkmar, R. Apostolov, M. R. Shirts, J. C. Smith, P. M. Kasson, D. van der Spoel *et al.*, *Bioinformatics* **29**, 845 (2013).
- [56] See Supplemental Material at <http://link.aps.org/supplemental/10.1103/PhysRevB.97.075115> for details on the calculated energy values.
- [57] P. Wzietek, H. Mayaffre, D. Jérôme, and S. Brazovskii, *J. Phys. I France* **6**, 2011 (1996).
- [58] We note that a steplike increase in $C(T)$ is related to a steplike change of $\alpha_i(T)$ via the Grüneisen relation. However, the sign of the anomalous contribution to $\alpha_i(T)$ is given by the Grüneisen parameter, i.e., by the pressure dependence of the corresponding energy scale.
- [59] P. Nagel, V. Pasler, C. Meingast, A. I. Rykov, and S. Tajima, *Phys. Rev. Lett.* **85**, 2376 (2000).
- [60] M. de Souza and L. Bartosch, *J. Phys.: Condens. Matter* **27**, 053203 (2015).
- [61] A. L. Goodwin, M. Calleja, M. J. Conterio, M. T. Dove, J. S. O. Evans, D. A. Keen, L. Peters, and M. G. Tucker, *Science* **319**, 794 (2008).
- [62] A. L. Goodwin and C. J. Kepert, *Phys. Rev. B* **71**, 140301 (2005).